

Paving the path toward silicon as anode material for future solid-state batteries

Palanivel Molaiyan^{a,*,*,1}, Buket Boz^{b,1}, Glaydson Simoes dos Reis^{c,d,1}, Rafal Sliz^e, Shuo Wang^{f,g,*,*,1}, Marco Borsari^h, Ulla Lassi^a, Andrea Paoletta^{h,*} 

^a Research Unit of Sustainable Chemistry, University of Oulu, Pentti Kaiteran katu 1, P.O.Box 8000, FI-90014, Oulu, Finland

^b Battery Technologies, Center for Low-Emission Transport, Austrian Institute of Technology (AIT) GmbH, Giefinggasse 2, 1210, Vienna, Austria

^c Laboratory of Industrial Chemistry and Reaction Engineering, Faculty of Science and Engineering, Åbo Akademi University, 20500, Åbo/Turku, Finland

^d Department of Forest Biomaterials and Technology, Swedish University of Agricultural Sciences, Biomass Technology Centre, SE-901 83, Umeå, Sweden

^e Optoelectronics and Measurement Techniques Unit, University of Oulu, FI-90570, Oulu, Finland

^f Center of Smart Materials and Devices, State Key Laboratory of Advanced Technology for Materials Synthesis and Processing, School of Material Science and Engineering, Wuhan University of Technology, Wuhan, 430070, China

^g Foshan (Southern China) Institute for New Materials, Foshan, 528200, China

^h Department of Chemical and Geological Sciences, University of Modena and Reggio Emilia, Via Campi 103, 41125, Modena, Italy

ARTICLE INFO

Keywords:

Silicon anode
Solid-state batteries
Anode materials
Solid electrolyte interface
Solid electrolytes

ABSTRACT

Solid-state batteries (SSBs) have emerged as an important technology for powering future electric vehicles and other applications due to their potential for enhanced safety and higher energy density compared to lithium-ion batteries (LIBs). Among future energy storage systems, SSBs (either semi or full SSBs) are the most promising candidates in terms of safety, cost, performance, and compactness. There has been a great effort to utilize silicon (Si) anode in SSBs due to its high specific capacity (3590 mAh g^{-1}), low cost, and earth abundance. SSBs with silicon anodes displayed attractive application prospects. The current research efforts showed that there is a great need to understand electrochemical performance, especially the interphase behavior, Si material design, and advanced tools for analytical characterization. In this review, we provide insights about the Si anode design, interface issues, SEI formation, failure mechanisms, and material modifications for the development of next-generation Si-based SSBs of use to bridge the gap between applied research and industrial scale applications.

1. Introduction

The climate crisis and driving the shift to electric mobility are the fast-growing need for safe and affordable high-capacity and high-energy storage batteries [1]. This green energy revolution lies under an equally impressive evolution in battery technology. Over the past decade, lithium-ion batteries (LIBs) have surpassed expectations to deal with the global climate goals that require even more significant improvements [2]. To date, LIB technology could provide only incremental performance gains with the theoretical limits. Hence, LIBs may not be enough to meet the requirements of cheaper EVs with extended driving range, longer battery life, high-temperature operation, and fast charging

infrastructure [3–6].

Currently, solid-state batteries (SSBs) have attracted great attention owing to their high safety and increased energy density and are considered the most promising next-generation batteries (Fig. 1a) [7,8]. SSBs are expected to be a game-changing technology for accelerating the popularity of EVs and other applications, due to their higher energy density which is twice as high as the conventional LIBs, as well as the lower cost thanks to the opportunity of using less expensive raw materials such as silicon as efficient electrodes [7,9,10]. In contrast with traditional LIBs, SSBs have a solid electrolyte (SE) that separates the anode and cathode electrode battery [11]. By replacing traditional graphite anodes with lithium metal or silicon-based anodes (Si), SSBs

* Corresponding author.

** Corresponding author.

*** Corresponding author. Center of Smart Materials and Devices, State Key Laboratory of Advanced Technology for Materials Synthesis and Processing, School of Material Science and Engineering, Wuhan University of Technology, Wuhan, 430070, China.

E-mail addresses: palanivel.molaiyan@oulu.fi (P. Molaiyan), shuowang@whut.edu.cn (S. Wang), andrea.paoletta@unimore.it (A. Paoletta).

¹ The authors equally contributed to the manuscript.

can offer enhanced energy density and thermal safety (Fig. 1b).

A key aspect of the promise of SSBs is that the all-solid-state architecture could provide custom design advantages to enable the reliable use of high-capacity electrode materials beyond those used in LIBs. Fig. 1c represents the recent developments for Si anode materials for LIBs and SSB. According to the resources, 8 million tons of Si could be yearly produced at a price that is 8 times lower than that for the production of 0.082 million tons of Li (\$2100 per ton of Si and \$17,000 per ton of battery-grade lithium carbonate, Fig. 1d) [12]. Si-based SSBs (cathode NMC811//sulfide SE//Si) show gravimetric (356 Wh kg⁻¹) and volumetric (965 Wh L⁻¹) energy density values that are comparable to those obtained using (cathode NMC811//sulfide SE//Li) Li metal anode (410 Wh kg⁻¹ and 928 Wh L⁻¹, respectively), great improvements could be achieved on costs, processability (scalability), safety, and electrochemical performances when Si anode is implemented in the cells [13,14]. Compared to the Li metal counterpart, Si-based SSB can

withstand high stacking pressure to improve the contact between electrode and electrolyte and operate at room temperature. This could improve safety (suppression of short circuits) and electrochemical (faster reaction kinetics) performances [12,15–17]. Furthermore, higher ionic conductivity could also be achieved in Si-based composite anodes as these anodes showed enhanced thermodynamic stability with the majority of solid electrolytes (e.g. sulfide-based solid electrolytes) [18, 19]. In this review article, we aimed to discuss in detail the electro-chemo-mechanical behavior of Si-based anode materials for SSBs, including the lithiation mechanism, volume expansion behavior, and SEI formation of the Si-based SSB, solid electrolytes design, as well as their evolution and effect of stress connected with its failure mechanisms. In addition, we comprehensively summarize the recent research progress of Si-based SSBs, which could provide advanced optimization strategies for further constructing long-cycle and high-energy-density SSBs. We also present prospects related to the possibilities for

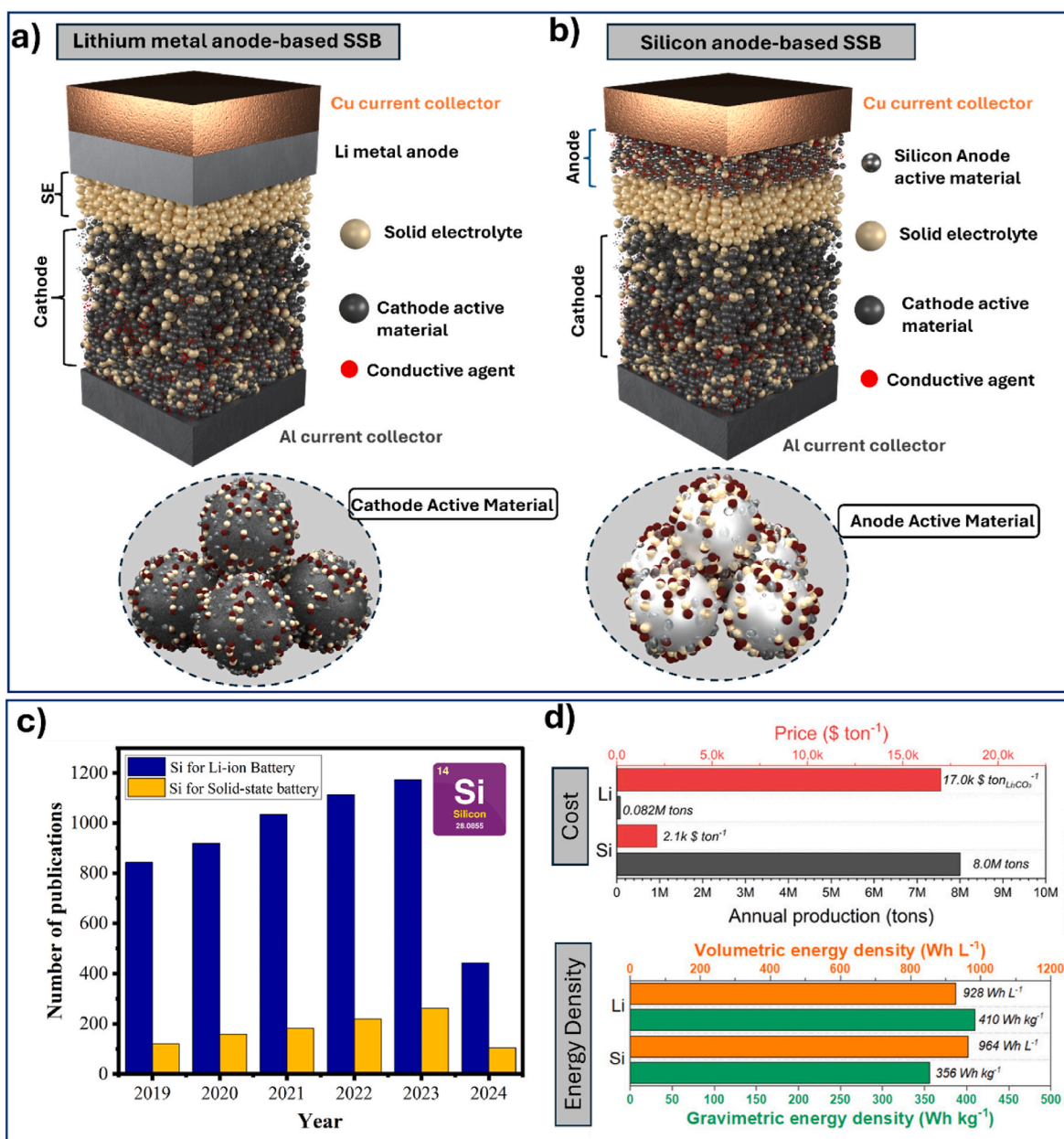


Fig. 1. a) A schematic architecture of Li metal anode-based SSB and b) Silicon anode-based SSB. c) Number of published articles from 2019 to 2024 for “Silicon” and “solid-state battery” (Web Source: Scopus). A total of 6570 research publications, 5524 for Lithium-ion battery and 1046 for solid-state battery. d) A comparison of cost and energy density for Li and Si anodes for SSBs (NMC811 as a cathode, Sulfide as a solid electrolyte) [12].

commercializing Si-based anodes for SSB.

2. Different types of anodes for SSB and the role of solid electrolyte interface (SEI)

SSBs are set to be the next-generation technology for high-performance batteries with improved safety and high energy density. However, the lack of suitable high-capacity electrodes for high-performance SSBs with stable long-term cycling hinders the full SSB implementation. In addition to the Li metal, various kinds of negative anodes show that materials such as silicon (Si), carbon (C), aluminum (Al), graphite (Gr), bismuth (Bi), lithium titanate (LTO), and tin (Sn) are considered as suitable candidates for high-performance and high capacities SSB cells (Fig. 2a) [20–29]. These materials are particularly interesting as they could alloy with Li, which can potentially offer benefits compared to other anodes such as Li-metal foils and anode-free Li-metal [30]. They help to avoid failure mechanisms, dendrite growth, and short-circuiting (Fig. 2b). Alloy anode materials including Si, Sn, and Al could boost the storage of the amount of Li^+ compared to graphite anodes [31], and when used in SSBs can deliver, higher specific energy and energy density values [14]. The predicted energy density values for alloy-based SSBs are closer to those for Li-metal SSBs. In addition to energy density values, alloy anodes can alleviate the abovementioned degradation issues related to Li metal. Thus, alloying is a good strategy for achieving high-density energy SSBs by overcoming the issues related to the Li-metal anode.

As an example of a next-generation anode material that could be enabled within SSBs, lithium metal (Li) and Si anodes have received considerable attention. Most widely, Li metal is considered the most promising anode material for SSBs due to its extremely high theoretical specific capacity ($\sim 3860 \text{ mAh g}^{-1}$), which is more than ten times higher than that for graphite anode (372 mAh g^{-1}) used in commercial LIBs [30,32]. It has the lowest negative potential (-3.040 V vs. standard hydrogen electrode (SHE)), which leads to a high output voltage during operation. Unfortunately, Li metal anode faces many issues regarding the formation of dendrites at high current densities, dead Li, and volume expansion which hinder its practical application due to huge capacity losses and safety risks [33]. During charging, Li forms dendrites and when the dendrites grow bigger it causes a short circuit. A large current can pass through the system, which can provoke a heat increase, resulting in safety risks or explosion [34,35]. Moreover, the physical and electronic detachment of these Li deposits (“dead Li”), provokes the rise of the battery’s internal resistance, leading to the higher consumption of

active substances (electrolytes), which diminish the battery capacity, volume expansion, and CE [36,37]. This volume expansion results in interface fluctuation as well as internal pressure change, which leads to the partial or total destruction of the solid electrolyte interphase (SEI), therefore reducing the stability and performance of the anode due to the low CE and high resistance.

Interestingly, Si-based anodes gaining more attention towards SSB due to their abundance of the raw material (leading to potentially low production costs), environmentally benign nature at the macroscale, high theoretical specific capacity ($\sim 3590 \text{ mAh g}^{-1}$), and low operating voltage versus Li (compared to other alloy anodes), are considered as valuable choice as alternative anode material [38]. A functional SEI plays a big role in the Si anode composite electrodes in SSB and LIB (Fig. 3). The evolution of SEI on Si is complex due to the large volumetric changes (300 %) during lithiation and delithiation. However, the volume expansion-contraction poses the following challenges: (a) the SEI layer undergoes continuous modifications during cycling, exposing fresh Si surface to the electrolyte and formation of new SEI. Thus, a gradual increase in the SEI layer thickness and electrolyte consumption is observed, leading to capacity retention. (b) The volume expansion also creates large stresses on the silicon particle itself resulting in the anode pulverization, trapping Li^+ ions in the anode host due to reduced diffusion across different particles. (c) The pulverization and volume expansion/contraction further contribute to delamination and/or loss of electrical contact with the current collector leading to a rapid capacity drop after a few cycles [39].

The research on the understanding of the SEI layer on conventional LIBs is highly advanced whilst, there is still an extensive effort to gain a better understanding of the SEI components. The SEI layer forms due to the precipitation of decomposition products derived from the reduction of solvents, salts, and impurities at the anode potential operating window [42]. Therefore, the electrolyte composition especially, the solvation shell of Li^+ which partially decomposes, plays a crucial role in the SEI layer formation. An optimized SEI layer is expected to have negligible low electronic conductivity while having high Li^+ selectivity and permeability. Once it is properly formed, further decompositions of salts and solvents are prevented since the electrons cannot transfer to or through the layer (the increased electronic resistance increases the potential on the Gr surface and shifts the surface potential within the stability window of the electrolyte). SEI on Si anode with conventional carbonate electrolyte consists of a combination of lithium silicate (Li_xSiO_y), lithium carbonate (Li_2CO_3), lithium fluoride (LiF), and other decomposition products of electrolytes such as lithium alkyl carbonates

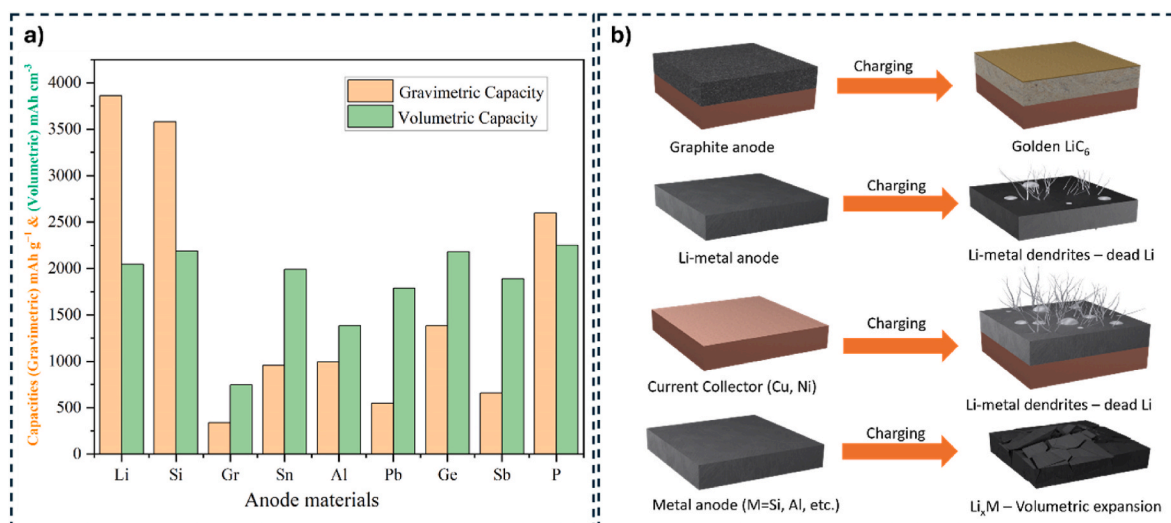


Fig. 2. a) Capacities of different anode materials for LIB and SSB applications. b) A schematic of different anodes behaviours during the charging process and related problems.

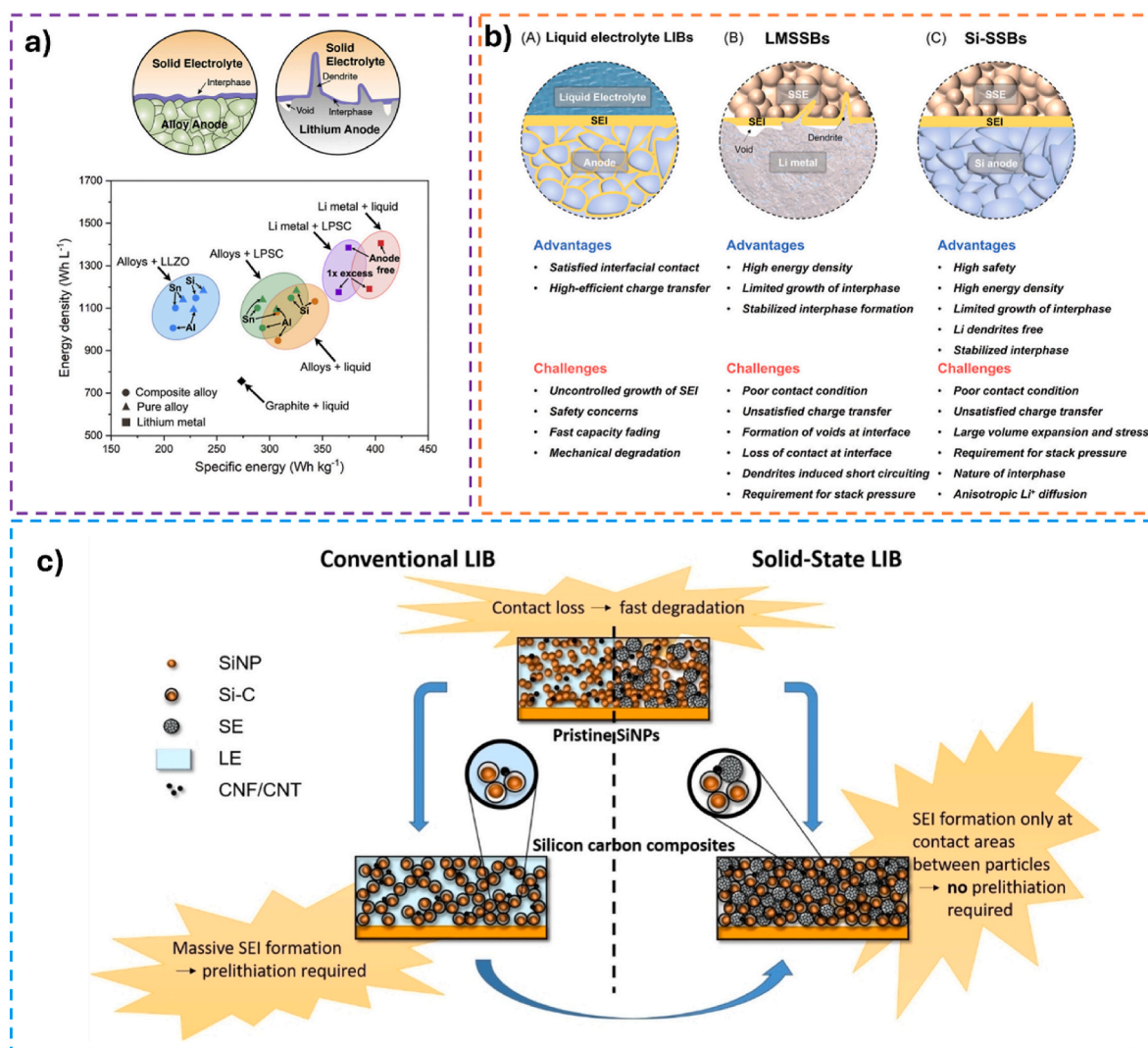


Fig. 3. i) A different type of anode materials for SSBs and LIBs with the prediction energy density. The interphase formation with SEs based on Si and Li metal anodes in SSB [20]. ii) Advantages and disadvantages of different anode materials for LIBs and SSBs and their SEI formation [40]. iii) Illustration of Silicon nanoparticles and Si-C based anodes for LIBs and SSBs [41].

like the LIBs [43]. SEI has been investigated thoroughly on conventional anode whereas, a comprehensive understanding of Si anode is still missing (Fig. 3iii). In liquid electrolyte applications, Si anode shows particle pulverization and continuous SEI formation which leads to severe loss of lithium inventory. However, Si anode in SSBs might show less or different SEI formation and particle pulverization because of the mechanical rigidity of inorganic SE and external stack pressure [44].

Substantial research has been devoted to improving SEI performance by using electrolyte additives [45,46], encapsulating Si particles [47, 48], and artificial surface layers [49,50]. A large variety of characterization techniques such as electrochemical impedance spectroscopy, Raman spectroscopy, atomic force microscopy, and X-ray photoelectron spectroscopy have been employed to comprehend the functionality of SEI [51–54]. Its feature which regulates the interaction between the silicon particles and the charge carriers, is of primary importance for the performance of the anode. The SEI layer on the Si anode would experience high local strain owing to the large volume expansion of Si particles during the lithiation process. As a consequence, SEI layers with a low modulus tend to suffer from severe local deformation and even fracture, which would reveal the internal Si granules and then lead to further generation of a thick SEI or even “dead Si”. Thus, a stable SEI could help in stabilizing the Si anode during the lithiation process to prevent some of the mentioned issues.

3. Importance of solid electrolytes coupled with Si anode for SSB

Electrolytes ensure the shuttling of ions from one electrode to the other upon cycling, allowing redox reactions to occur. A suitable electrolyte candidate must exhibit high ionic conductivity, and negligible electronic conductivity, and must be electrochemically stable within the operating voltage of the cell. The most widely used organic liquid electrolytes (LEs) are carbonate-based with lithium salt which has the drawbacks of being volatile and flammable. The leakage of the LEs, as well as the internal short circuit caused by dendrites and the performance, is one of the main issues that current LIBs are facing. The technology of SEs is currently one of the first methods to prevent the growth of dendrites for SSBs. Thus, in recent years, pairing SEs with alloy anode has shown promising results in preventing those issues. The nature of SSBs depicts entirely different interfacial dynamics than the liquid electrolyte. At the interface between an alloy active material and an SE, the SE does not flow to continually wet the alloy material surface during volume changes. This will likely result in a reduced extent of SEI formation compared to alloys in liquid electrolytes [20,46,55]. SEs are promising candidates for next-generation SSBs with benefits of safety, energy density, low cost, and mechanical and thermal stabilities. SEs can be divided into four chemistries; sulfides, halides, oxides, and polymers [8]. Sulfide solid electrolytes (SSEs) have high ionic conductivity as they

can form a wider interface area between the electrode and electrolyte. Despite the oxide-based electrolytes showing lower ionic conductivity than sulfide electrolytes, they have high electrochemical stability [56]. Polymer-based electrolytes are versatile and have price competitiveness since they share similar properties and manufacturing processes with liquid electrolytes. Recently, halide-based SEs have drawn more attention for SSB applications due to processibility and high ionic conductivity. However, both halide and sulfide-based SEs are air-sensitive. The processibility of these electrolytes highly depends on the ambient conditions.

As mentioned, Si is considered a promising anode material for SSB due to its unique properties in overcoming the main challenges

associated with Li metal anodes (dendrite formation and morphological instability) [13]. Compared with Li metal anodes, Si anodes show higher stability against lithium argyrodites, and higher mechanical strength to effectively avoid the formation of lithium dendrites, which is regarded as one of the ideal anode materials for SSBs with long cycle life and high capacity at high C-rates [57]. Despite these positive attributes, there is a limited number of Si anode composites that have been implemented in SSB applications. This section will cover the SEs role for the Si anode in the SSB applications.

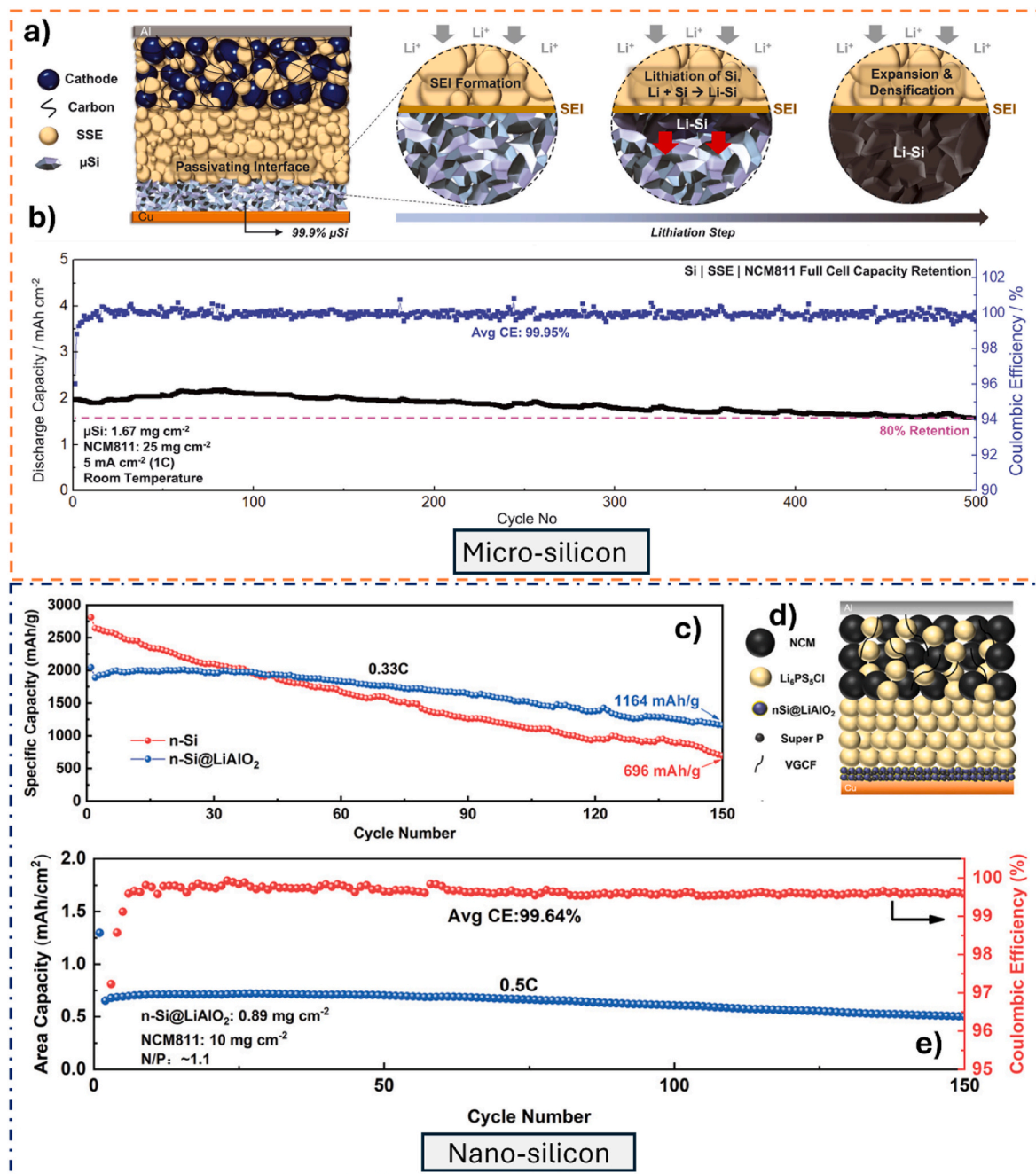


Fig. 4. a) A schematic representation for SSBs consists of a cathode composite layer, a sulfide solid electrolyte, and a micro-silicon anode. The lithiation process during the charging cycle forms Silicon alloy (Li-Si) particles. b) The electrochemical performance of $\mu\text{Si}|\text{SSE}|\text{NCM811}$ at room temperature (current rate of 1 C) [62]. c) The half-cell SSB cycling performance of Si and Si@LiAlO₂ electrodes at 0.33C for 150 cycles. d) Schematic diagram of nano Si@LiAlO₂/NCM. e) Long-term cycle performance of Si@LiAlO₂/NCM811@Li₂SiO_x at a current rate of 0.5C for 150 cycles (1 C = 200 mA g^{-1}) [63].

3.1. Sulfide-based solid electrolytes SEs (SSEs)

SSEs have exceptionally high ion conductivity in the range of 10^{-4} to 10^{-2} S cm^{-1} at room temperature and it is applicable for SSBs are anticipated. SSEs are promising candidates for SSBs not only high ionic conductivity but also full electrochemical windows, excellent mechanical properties, and easy reproducibility. However, many challenges towards SSEs remain to escalate difficulty in forming an optimized Li and SE interface offering fast Li^+ ion transport for SSB operation and minimizing electronic conductivity to avoid continuous degradation [58]. The carbon's effect, the particle size of Si, and the depth of silicon's lithiation were discussed thoroughly with SSEs [45,57]. Generally, SSE exhibits a reduced extent of SEI formation compared to the liquid case [59,60]. Some of the SSE are known to form stable interphases at low potentials which suggests that stable long-term cyclability might be achieved easily with alloys in the SSE environment [20,61].

It is found that the carbon-free Si electrode will greatly reduce the decomposition of the lithium argyrodite compared with the conventional carbon-containing Si-based anode, thereby improving the initial Coulombic efficiency and rate performance of the cell. The electronic conductivity of micro-silicon (3×10^{-5} S cm^{-1}) is akin to most oxide cathode active materials. Therefore, micro-Si can be used as the anode without adding conductive carbon. Hence, the interface contacts between the lithium argyrodite layer and the micro-Si electrode become a two-dimensional plane. Meng's group et al. [62] reported the stable operation of a 99.9 wt% μ -Si anode for SSB, the μ -Si anode offers high stability and energy density, operating for 500 cycles with 1.5 mAh cm^{-2} at 1 C with a CE of 99.95 % (Fig. 4a–b). Despite the large volume expansion of micro-Si, the two-dimensional interface maintains its structure well during the lithiation process due to high stack pressure on the cell [46]. Applying MPa-level stack pressure on the Si-based SSBs could alleviate physical contact loss caused by large volume changes of silicon anode during cycling, and improve the cycling stability of the SSBs. However, bulky molds are needed to apply several hundreds of MPa pressure, which will reduce the energy density of the whole cell. Interestingly, a sheet-type Si anode modified with LiAlO_2 layer-coated Si (Si@LiAlO_2) delivers the specific capacity of 1205 mAh g^{-1} (150 cycles, 0.33C) with a CE of 80 %. Full cell testing based on single crystal NCM83@LNO//SEs//Si@LiAlO₂ showed a reversible capacity of 147 mAh g^{-1} (0.28 mA cm^{-2}) and a capacity retention of 80.2 % (62 cycles, 1 C) (Fig. 4c–d) [63]. The enhanced electrochemical performance is attributed to the improved Li^+ diffusion kinetics in the electrodes and the lower expansion ratio of the electrode. The calcined LiNO_3 , asphalt (as the source of carbon), and Si nanoparticles (around 2–8 μm) form micro-Si@Li₃PO₄@C anode material [64].

The Micro-Si@Li₃PO₄@C anode proved to be highly effective in SSBs due to the synergistic effect of Li₃PO₄ and carbon incorporation that replenished Li and CE was higher than that of nano-Si, suggesting the important role of the structural anode design. The anode material was used in the full cell with NMC111 in 3D-PPLLP-CPEs being able to maintain a capacity of 129.2 mAh g^{-1} at 0.2C with 98.5 % capacity retention after 100 cycles. The authors reported that after cycling, the anode material remained intact over the copper foil, and no cracks were observed. The capacity of the Micro-Si@Li₃PO₄@C showed high values, which are higher than those of many reports dealing with Si-based SSB anodes.

To understand more about the nano-Si composite anode role in SSB [65], nano-Si composite was prepared by ball milling method mixing Si powder, SSE like Li_{5.4}PS_{4.4}Cl_{1.6}, and carbon black. The anode is composed of three components (Si–SE–C) that are chemically stable. The addition of SE and carbon to Si provides excellent electron and ion conduction pathways in the Si–SE–C anode composite. Interestingly after delithiation, the Si, once crystalline, became amorphous, and the existence of SE and carbon enables an integrated electrode with less void formation. When no carbon is used to alleviate the volume expansion Si–SE, voids appear in the Si–SE anode due to a change in its volume,

which triggers the degradation of the anode and consequently capacity loss of the SSB. The anode behavior of pure Si, as the only phase, the electron conduction and ion diffusion rely only on Si that are lower than Si–SE and Si–SE–C anodes. Thus, the kinetic is limited and it suffers a huge volume expansion since there are no buffers (carbon and SE) to alleviate it. At the beginning of the delithiation process, voids appear and the whole anode collapses along with the SSB.

Han's group [66] studied the effect of three different SEs (sulfide (LPS), iodide-substituted sulfide (LPSI), and hydride-based (LBHI)) on the ICE of Si-based anodes in SSBs. The results demonstrated that LPS and LPSI showed apparent decomposition during the Si-anodes charge/discharge exhibiting poor CE (75.9 %, LPS, and 77.6 %, LPSI). The poor stability was associated with side-reactions between Si and P (present in SSEs). However, regarding LBHI electrolytes, no apparent electrochemical decomposition was observed, achieving an outstanding electrochemical/chemical stability yielding a CE of 96.2 %. The full cells with the LBHI-based SEs reported the highest discharge capacity of 152 mAh g^{-1} at 0.5C and much better cycling stability than LPS and LPSI.

Two different Si-based anodes micron-sized (μSi) and SiNWs utilize and demonstrated and could be able to obtain the specific capacity of 2700 mAh g^{-1} and 2600 mAh g^{-1} for SiNW: after 15 cycles, the loss in capacity was due to the irreversible formation of SEI, which was related to the area of active material exposed to the SEs [67].

The interfaces between Si composite anode and lithium argyrodite (LPSCI) leads to continuous interfacial side reactions. Therefore, the current challenges need to be solved for the Si-based SSBs: (i) improve the ion/electron conducting pathway of the composite anode. (ii) stabilize the Li-Si/SSE interface to prevent continued SEI growth and accumulation of dead silicon particles. In general, composite anodes in SSBs are usually prepared by mixing Si composite anode with electron conductive additive, lithium argyrodite, and binder. To optimize the ionic and electronic transport pathway in the composite anode, the amount of inactive components is usually increased, which reduces the volume and gravimetric energy density at the electrode level. The conductive pathways are easily disrupted by the expansion and contraction of the Si composite anode, resulting in irreversible segregation between particles and rapid capacity loss of the cell during cycling [68,69]. Therefore, constructing a robust high-capacity Si-based anode with high ionic/electronic transport pathways is essential for the commercialization of high-energy-density SSBs.

The particle size distribution of Si has a great influence on the electrochemical performance of the SSBs. Larger particles force structural deformation throughout the electrode during cycling, while smaller particles can more easily fill the available pores within the composite anode, leading to a small volume change of the composite anode, which alleviates the mechano-electrochemical failure [70]. The surface of nano-Si particles is usually covered with a layer of silicon oxide, which reduces the electronic conductivity by three orders of magnitude. Since nano-Si has a larger surface area, the composite anode prepared via ball milling the mixture of nano-Si, conductive carbon, and lithium argyrodite can improve the utilization of nano-Si (Fig. 5a) [12]. Similar to the injection of liquid electrolyte into commercial LIBs, the precursor of lithium argyrodite can be infiltrated into the Si/carbon/binder composite anode sheet to increase the contact area between Si active material and lithium argyrodite, thereby improving the ionic transport pathways in the composite anode [71].

To accommodate the volume change of Si, carbon nanofibers (CNFs) with good mechanical properties are ideal matrices for Si nanoparticles. The stress relaxation and robust electronic pathways can be achieved by embedding Si nanoparticles in CNFs. Coating lithium argyrodites on the Si/CNF surface by a simple liquid-phase method can enlarge the contact area between solid electrolyte and Si anode, provide more electrochemical active sites, improve ionic transport pathways, and enhance reaction kinetics, which finally enables high utilization of Si [72]. The graphite is also a good matrix to distribute the nano-Si powder. The mechanically flexible graphite continuously provides abundant

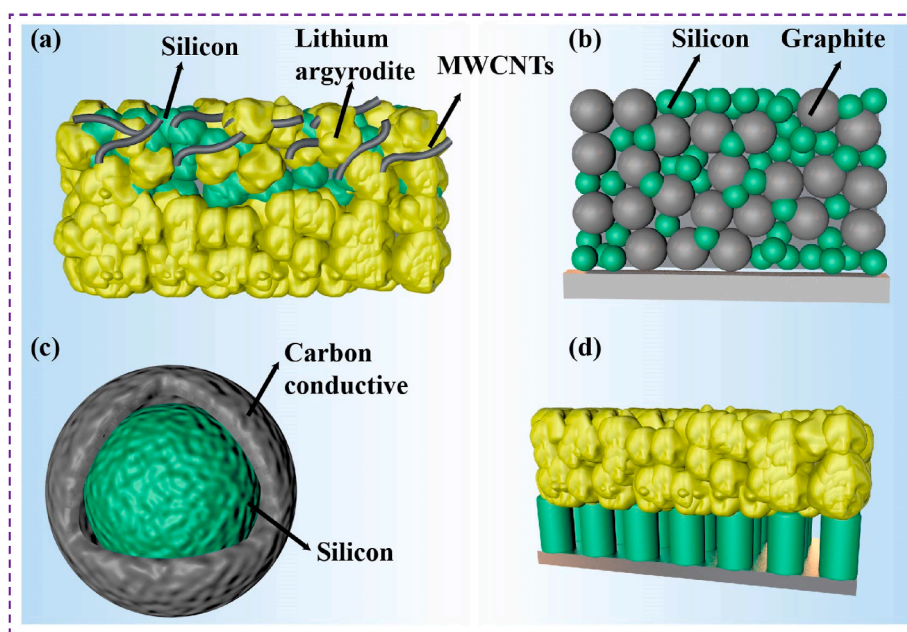


Fig. 5. (a) Silicon-lithium argyrodite-MWCNTs composite anode via ball-milling; (b) graphite-silicon composite anode; silicon-carbon anode with core-shell structure; (d) columnar silicon anode for stabilizing the silicon/lithium argyrodite interface.

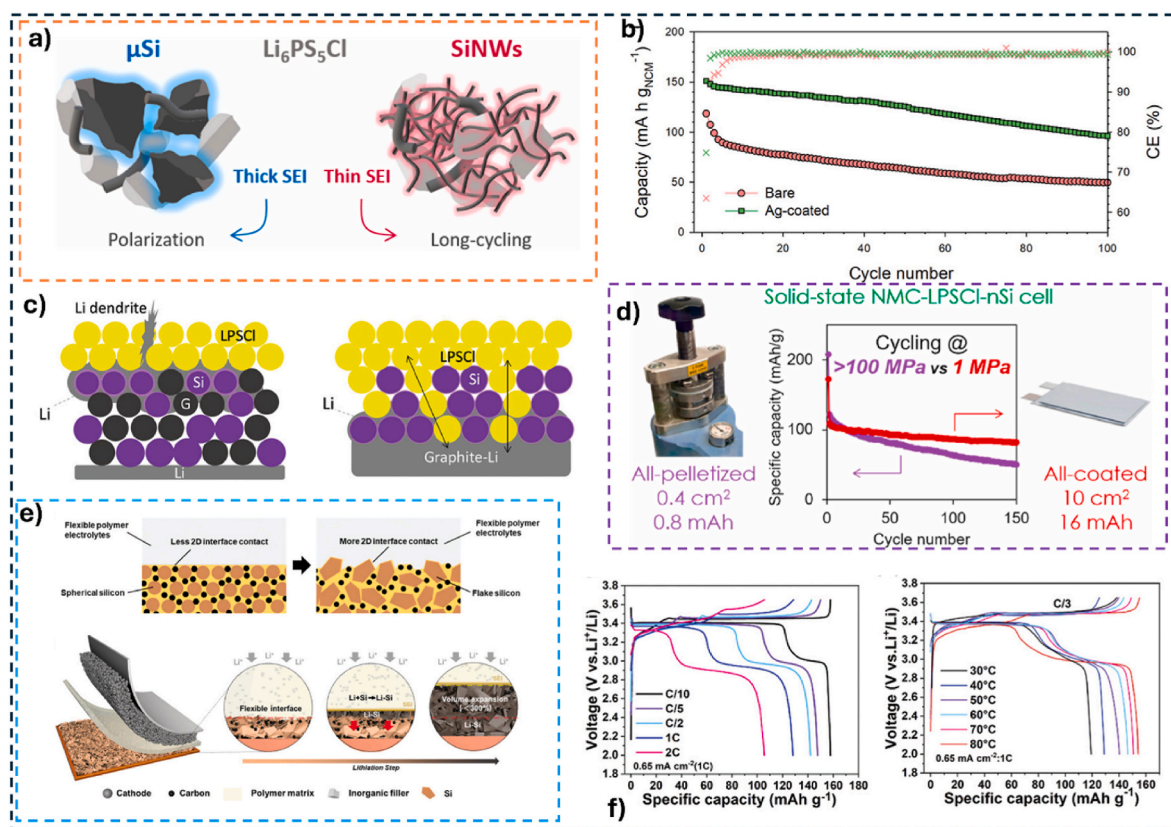


Fig. 6. a) A schematic representation of SEI formation with two different Si anodes (SiNW and micro-Si) [67]. b) The electrochemical performance of bare and Ag-coated Si electrodes with NCM cells under 15 MPa and 30 °C at a current rate of 0.2C [73]. c) Illustration of the effect of Si composite anode (LPSCl mixed with Si) to better transport Li toward the current collector to prevent Li dendrite penetration, in comparison without LPSCl SSE mixed in the Si-graphite layer (left panel) [75]. d) Cycling performance of all-coated cells nSi/LPSCl/NMC pouch cells under two different pressures (1 MPa, red color) and coated-pelletized cells (125 MPa, blue color) [74]. e) Schematic diagram of spherical and flake Si anode with composite polymer SE. An SSB full cell, lithiation process of Si-based electrode and composite SE. f) The cycling performance of the Si//PHP-L15/LiFePO₄ with various current rates as well as the different temperature tests at 0.33C [76].

electrons for Si, resulting in a stable electrochemical reaction. Utilizing nano-Si powder could increase the interdiffusion area between graphite and Si, and also shorten the diffusion path, thereby increasing the power density of SSBs (Fig. 5b) [19]. Preparing Si-carbon composites with a core-shell structure can not only effectively compensate for the volume change of silicon during cycling, but also the carbon shell could increase the electronic conductivity of the composite anode and the stability of the SEI layer formed on the carbon shell (Fig. 5c) [41]. Similar to the utilization of a layer of micro-Si, using a columnar silicon anode could also help to form a two-dimensional SEI layer when in contact with lithium argyrodites, which will reduce the side reactions (Fig. 5d) [60].

Strategies to overcome the interface issue instability between SSE ($\text{Li}_6\text{PS}_5\text{Cl}$) and Si-based electrodes have been reported [73]. To tackle the unstable interface issue, a metallic silver (Ag) as an adhesive inter-layer which alloys with Li during the cycling, and retains deformable characteristics, reducing the damage of the cell due to the less volume expansion; moreover, it provides a good Li^+ transportation across the Si/SE interface, even under high dimensional changes in the Si-based electrodes. The Ag-coated Si anode-based SSB specific capacity was much larger than that for bare Si anode (151 vs 119 $\text{mAh g}_{\text{NCM}}^{-1}$) and the capacity retentions of 64 % and 42 % after 100 cycles, respectively (Fig. 6). The modification of coating Ag on Si anode seemed to be highly effective for improving the stability and electrochemical performances

of the electrodes and overcoming interface issues. A promising and scalable Si-SSB strategy was through pouch cells (pelletized 7 mm-diameter molds of 10 cm^2), whereas an LPSCl layer as a separator with NCM cathode [74]. The densified cell was under a pressure of 390 MPa and 1 MPa, the lower pressure maintained a high stability over 160 cycles at room temperature. This approach opens the gateway to overcome the main failure mechanisms involved in Si-based SSBs, especially tackling the issue related to fast capacity decay.

To obtain insights into possible SSB failure mechanisms, chemo-mechanical failure mechanisms of Si/ $\text{Li}_6\text{PS}_5\text{Cl}$ composite and solid-electrolyte-free silicon anodes were investigated [44]. The growth of the SEI at the Si/ $\text{Li}_6\text{PS}_5\text{Cl}$ interface was found to trigger a large resistance increase in composite anodes. The fast battery capacity decay was directly due to the high resistance. The presence of oxygen can cause issues for the anode performance due to the reaction with Si to form SiO_x , which has implications for the continuous growth of the SEI. An efficient composite anode is made by mixing SE with Si-nanoparticles in one layer and using graphite as a separation layer to the Li metal layer [75]. This strategy resulted in less lithiation of Si due to the Li^+ transportation through the SE in the Si-layer and more Li plating toward the current collector, which gave a lower anode voltage, and thus, a higher battery voltage. This strategy provides new and effective design principles of fast SSB kinetics assuring elevated power densities with high

Table 1
Summary of the electrochemical performance of Si anode-based solid-state batteries.

Cell configurations			Temp.	Voltage (V) (vs. Li^+/Li)	Active materials loading	Current density	Initial cycle Performance	Cycle life	Capacity retention	Ref.
Anode composition	solid electrolyte	cathode composition								
Si/ $\text{Li}_6\text{PS}_5\text{Cl}$ /CB	$\text{Li}_6\text{PS}_5\text{Cl}$	NCM811@ Li_2SiO_x	30 °C	2.4–4.2	NCM811: 10 mg cm^{-2}	0.3C	145 mAh g^{-1} at 1st discharge	91 mAh g^{-1} after 1000 cycles	–	[12]
Si/C	$\text{Li}_6\text{PS}_5\text{Cl}$	NCM90	RT	1.5–4.25	Si-C loading: 4.8 mg cm^{-2} , $n/p = 2$	0.2 mA cm^{-2} and 1.0 mA cm^{-2}	125 mAh g^{-1} at 1st discharge	109 mAh g^{-1} after 52 cycles	87.7 %	[41]
columnar Si	$\text{Li}_6\text{PS}_5\text{Cl}$	NCM90	25 °C	2.0–4.0	Si: 1.0 mg cm^{-2} NCM811: 12.8 mg cm^{-2}	1 mA cm^{-2}	143 mAh g^{-1} at initial discharge,	118 mAh g^{-1} after 50 cycles	82 %	[60]
μSi -PVDF	$\text{Li}_6\text{PS}_5\text{Cl}$	NCM811	RT	2.0–4.3	μSi : 1.67 mg cm^{-2} NCM811: 25 mg cm^{-2}	5 mA cm^{-2} (1 C)	~1.875 mAh cm^{-2} at initial discharge	~1.5 mAh cm^{-2} after 500 cycles	80 %	[62]
Li-In//SE//Si-PAN	$\text{Li}_6\text{PS}_5\text{Cl}/77.5\text{Li}_2\text{S}-22.5\text{P}_2\text{S}_5$	–	60 °C	0.1–1	Si: 0.9 mg cm^{-2}	Initial 0.05C, following 0.1C	1606 mAh g^{-1} at initial discharge	1122 mAh g^{-1} after 200 cycles	70 %	[70]
$\text{Li}_6\text{PS}_5\text{Cl}$ -infiltrated Si/C/PVDF	$\text{Li}_6\text{PS}_5\text{Cl}$	LCO	30 °C	2.8–4.2	LCO loading: 10 mg cm^{-2}	0.1C (0.14 mA cm^{-2})	104 mAh g^{-1} at 1st discharge	–	–	[71]
Li-In//SE//Si/C/ $\text{Li}_6\text{PS}_5\text{Cl}$	$\text{Li}_6\text{PS}_5\text{Cl}$	–	25 °C	0.05–1.5	Si loading: 1.54 mg cm^{-2}	0.5C	728 mAh g^{-1} at 1st discharge,	607 mAh g^{-1} after 50 cycles	83.4 %	[72]
Si	$\text{Li}_{2.6}\text{Zr}_{0.4}\text{Lu}_{0.6}\text{Cl}_6$	NCM85	RT	2–4.3	Si: 2 mg cm^{-2} NCM85: 25.46 mg cm^{-2}	0.5C	3 mAh cm^{-2} at 1st discharge	2.5 mAh cm^{-2} after 1500 cycles	80 %	[85]
Si/ $\text{Li}_6\text{PS}_5\text{Cl}$ /C	$\text{Li}_6\text{PS}_5\text{Cl}$	NCM811	RT	2.4–4.1	Si: 0.7 mg cm^{-2} NCM811: 18.9 mg cm^{-2}	0.1C (0.24 mA cm^{-2})	1.8 mAh cm^{-2} at initial discharge	1.1–1.2 mAh cm^{-2} after 100 cycles	64 %	[86]
Si@LLZTO//SE//Li	LLZTO	–	RT	0.01–3	–	1 A g^{-1}	1363 mAh g^{-1} at initial discharge	386 mAh g^{-1} (1000 cycles)	–	[87]
μSi @ MgO @C	PEO@LATP@NCF	LFP	RT	2.8–4.3	–	0.2C	104.5 mAh g^{-1} at initial discharge	70 mAh g^{-1} after 50 cycles	–	[88]
Si@MOF (ZIF-67)	PPG	LFP	60 °C	2.8–4.3	LFP: 3.5 mg cm^{-2}	0.5C	135 mAh g^{-1} at initial discharge	110 mAh g^{-1} after 50 cycles	73.1 %	[89]

cell stability over the long-cyclability. These are necessary steps to help clear the path for the larger-scale applications (Table 1).

Following innovative strategies to effectively synthesize different configurations/features and high-density capacity Si-based anodes for SSBs, a high CE over cycling is a crucial parameter for highly efficient SSBs, especially when Si-based anodes are employed. Many issues regarding sustaining high CE are related to the poor stability between SE/Si-anode. Another research that sophisticatedly employed a Si-anode was proposed by Na and coworkers [77]. The group successfully demonstrated that a pure Si-monolithic (void-free and additive-free) can be considered an efficient anode for high-performance SSBs. The Si-monolithic anode delivered a high areal capacity of 10 mAh cm⁻² (half-cell at room temperature) and 8.8 mAh cm⁻² (full-cell at 60 °C) at a current rate of 0.5 mA cm⁻². The high capacities were achieved thanks to the anode structural and geometric features, which enabled fast Li⁺ transportation across the electrode thickness combined with an even distribution of Li⁺ along the whole monolith.

Fan and colleagues [78] studied an in-situ pre-lithiation strategy to boost the performance of an electrolyte-free Si anode. The authors reported that the employment of a prelithiation process, by using an ultra-thin Li foil, provoked a significant improvement in the reversible capacity of the SSB due to improved Li intercalation kinetics. The cells showed a delivered energy density of 402 Wh kg⁻¹ at 0.1C (capacity retention of 57.3 % over more than 300 cycles at 0.5C). Overall, such a prelithiation strategy of electrolyte-free Si anode displays many advantages to addressing SSB issues that hinder its implementation by offering a pathway to develop high-energy-density SSBs. The same strategy of pre-lithiation was employed by Poetke and coworkers [79]. The partially lithiated (800 mAh g⁻¹) Si-microparticles led to a volume change in the order of only 66 % (instead of 300 %). This would avoid the anode pulverization caused by the severe expansion (300 %). The results indicated that the employment of Si partially lithiated in full cells exhibited energy densities up to 28 % higher than of commercial Gr anode.

The use of Si as an additive in an anode also composed of carbon material tailors the ionic and electronic transport throughout the electrode much faster and boosted the SSB metrics [80]. This will make the impact of Si particle size on SSB performance. It was found that the Si particle size (combined with SE) has a high impact on SSB rate performance, mainly due to the influence in the partial ionic and partial electronic transport, or composite tortuosity. Smaller Si particles enable the attainment of higher Si-anode/SE interface contact as well as improve the distribution of Si particles over the anode in a well-distributed compact packing in the compressed electrode. Thus, the modulation of the Si particle size can also be an efficient strategy for achieving high-performance anode materials for SSB.

3.2. Other SEs for Si-based SSB

In contrast with sulfide-based SEs dominating Si anodes for SSB, other solid electrolytes like oxide and polymer-based SEs are not investigated widely. The aim is to have more the options of employing polymer-based SEs for high-performance Si-anode materials for SSBs [81–83]. Ping and coworkers [25] found that a 1 μm thickness Si-based anode offers excellent contact with the SE and sustains good structural integrity during the Li-ion intercalation process. The anode delivered a high discharge capacity of 2685 mAh g⁻¹ (current density of 2.5 mA g⁻¹ (7 × 10⁻⁴ mA cm⁻²)) and sustained an excellent initial CE of 83.2 %. The conventional slurry coating method, and later impregnation with a polymer electrolyte (PE) which was solidified via thermal curing, was studied by Giffin and coworkers [84]. The results suggested that the capacity in Si/HPE/Li cells is highly dependent on the C-rate, areal capacity of the anodes, and SE/anode composition. The HPE containing LiFSI and no ionic liquids showed high-capacity retention and CE. It was stated that the anode which was composed of 75 wt% Si with a hybrid polymer electrolyte (also containing LiFSI and IL) exhibited a very high

capacity around 1500 mAh g_{Si}⁻¹ at 0.1C with a capacity retention of 74 % after 100 cycles. It was concluded that anodes with high Si contents showed better performances compared to those with less Si [85]. The garnet-type SEs for their compatibility with Si anode displayed a high discharge capacity of 2685 mAh g⁻¹ with a good initial CE of 83.2 % [25]. The ultrahigh loading pre-lithiated Si anode with halide-based SE Li_{3-x}Zr_x(Ho/Lu)_{1-x}Cl₆ demonstrated an areal capacity of 16.3 mAh cm⁻² [85]. Utilizing the composite ceramic mixed polymer-based SEs (PVDF-HFP/PEO/LATP15 % denoted as PHP-L15) pairing with Si-nanosheet anodes for SSBs also demonstrated promising outcomes [76]. The Si//PHP-L15//Li half cells showed excellent performance of reversible capacity of 817 mAh g⁻¹ after 200 cycles. In full-cell, LiFePO₄//PHP-L15//Si reported a high-capacity retention of 81 % after 100 cycles, and a rate capability of 105 mAh g⁻¹ at 2 C. In addition, PHP-L15 exhibited a high mechanical feature (tensile stress: 2.8 MPa; tensile strain: 40 %), which was responsible for limiting the evolution of the Si volume change, thus maintaining the integrity of the Si-based electrode and stable SEI film formation. Moreover, due to the inherent SE feature, the electrode displayed excellent flexibility and ductility, which could reach synchronously dynamic volume expansion/shrinkage among PHP-L15. The anode promoted a self-recovery of the SSB and created a suitable, stable, and effective interfacial contact with swift ions transfer during the long-cyclability processes.

3.3. Silicon-based full practical solid-state battery optimization

Since the surface of the silicon anode is typically covered by an oxide layer and silicon is a semiconductor, solid electrolytes, and conductive carbon are typically added to improve the reaction kinetics and electronic conductivity of the silicon anode. In order to enhance the areal capacity of the silicon-based composite anode, it is essential to minimize the content of inactive substances. In recent literature, the use of pure micron silicon (5 mAh cm⁻² [62]), the preparation of columnar silicon by physical vapor phase multiplication (3.5 mAh cm⁻² [60]), and the use of wafer silicon (10 mAh cm⁻² [77]) have been reported to achieve high areal capacity. However, due to the large volume change of silicon anode during cycling, silicon cracking occurs even under a large stacking pressure. Han et al. prepared the porous silicon decorated with Ag nanoparticles, covered with a layer of carbon, and combined the anode poly(vinylidene fluoride-co-hexafluoropropylene)/Li_{1.3}Al_{0.3}Ti_{1.7}(PO₄)₃ to assemble a half-cell. The cell achieves a high areal capacity of 4.0 mAh cm⁻² [45]. Zhang et al. prepared a Si-Li₂₁Si₅ anode and combined it with a LiCoO₂ electrode and Li₆PS₅Cl electrolyte to assemble an all-solid-state battery. The cell achieves a high areal capacity of 17.9 mAh cm⁻² at 55 °C [90].

In order to improve the energy density of the whole cell, it is necessary to optimize the N/P ratio, increase the active material loading in the composite cathode and anode, and reduce the thickness of the composite electrolyte membrane. Cao et al. mixed nano-silicon with Li₆PS₅Cl and CB to obtain a composite anode, and mixed Li₂SiO_x-coated LiNi_{0.8}Mn_{0.1}Co_{0.1}O₂ with Li₆PS₅Cl and VGCF to obtain a composite cathode, and prepared a Li₆PS₅Cl-ethyl cellulose composite electrolyte film by vacuum filtration. Finally, the three components were stacked to assemble a solid-state battery. When the cathode active material loading reached 20 mg cm⁻², the full battery could achieve a high energy density of 285 Wh kg⁻¹ [12]. They also tried bipolar stacking, and the energy density of the cell increased from 189 to 204 Wh kg⁻¹ compared with a single-layer battery [91]. Yan et al. prepared a hard carbon-stabilized Li-Si alloy anode, thus forming a three-dimensional ionic electronic conductive interconnect comprising plastically deformable lithium-rich phases (Li₁₅Si₄ and LiC₆). This could not only enhance the active area and alleviate stress concentration but also improve electrode kinetics and mechanical stability. The all-solid-state batteries combined with the LiNi_{0.8}Co_{0.1}Mn_{0.1}O₂ cathode and above anode were assembled. Even with a 650 μm-thick solid electrolyte layer, the cell still achieved an energy density of 263 Wh kg⁻¹ with a high areal loading of 20

mAh cm⁻² [92]. In summary, pure micron silicon is unsuitable as the anode material for SSBs because of its large volume change. Nano silicon-conductive carbon-sulfide-binder prepared by tape casting to obtain a composite anode will have great potential for large-scale application. The combination of Li-Si anode with hard carbon may be a promising avenue of research, but it will significantly increase the manufacturing cost of the battery (Fig. 7). In the future, it is necessary to develop a more viscous binder to achieve a strong silicon composite anode, thereby suppressing the volume expansion of the anode and achieving a long cycle life of silicon-based SSBs.

3.4. Prototype cells and startups of silicon-based solid-state batteries

Ionic Mineral Technologies has developed a silicon-graphite composite (i.e., 15 % pure silicon blended with graphite), which delivers a stable capacity of 600 mAh g⁻¹ for over 600 cycles [93]. Nexeon has replaced a small proportion of graphite with silicon to prepare a robust silicon-graphite hybrid electrode. This approach allows for the expansion of silicon within the structure, thereby alleviating capacity degradation and maintaining a good cycle life [94]. Amprius prepared silicon nanowires without binders and graphites. There is enough space between the nanowires and silicon porosity, which could accommodate silicon volume expansion. In addition, effective ionic and electronic transport pathways are established, leading to enhanced power capability and a rapid charge rate [95]. The specific capacity of BTR's third-generation silicon-carbon anode material has been enhanced to 1400 mAh g⁻¹, and the initial coulombic efficiency has been increased to 82 %. The production capacity of silicon-based anode materials has reached 6000 tons/year. Full production is expected to be achieved by 2028 [96].

Beijing WELION New Energy Technology Co., Ltd. has released a high-energy-density solid-state battery pack assembled with NCM811 cathode and graphite-silicon anode. The cells deliver an energy density of 250 Wh kg⁻¹ [97]. The GOTION HIGH-TECH Co., Ltd. has announced its first generation of "Jinshi" solid-state batteries with micro-nano solid electrolytes, a single crystal cathode coated with an ultra-thin film, and a three-dimensional mesoporous silicon anode. The cells achieve a high mass-energy density of 350 Wh kg⁻¹ and a volume energy density of 800 Wh L⁻¹, which is 40 % higher than the current mainstream ternary lithium-ion batteries in the industry. Furthermore, the cell shows a long-term cycling life of over 3000 cycles. The battery system constructed with Jinshi batteries exhibits an 80 % mass grouping rate and a system energy density of 280 Wh kg⁻¹ [98]. GAC Group has released a

new all-solid-state battery technology combining high-area capacity (5 mAh cm⁻²) solid-state cathode technology and third-generation sponge silicon anode technology. The cells achieve a high energy density of more than 400 Wh kg⁻¹. Compared with the current mass-produced commercial lithium-ion battery, the volume energy density is increased by more than 52 %, and the mass-energy density is increased by more than 50 %. Additionally, the battery can achieve no thermal runaway under conditions such as nailing and cutting and has passed the industry-leading 200 °C hot box test [99]. Solid Power has released a solid-state battery that uses a sulfide as a solid electrolyte, a high-content silicon as an anode, and NCM as a cathode. A high mass-energy density of 390 Wh kg⁻¹ and a volume energy density of 930 Wh L⁻¹ with a cycle life of more than 1000 cycles are obtained [100]. The above companies only released the energy density data of the SSBs. In the future, it would be better to show the cycling performance data to check the capacity retention and provide more parameters related to electrode materials. From single batteries to modules, and from quality control consistency to the engineering of the entire process, there is still much to be done in the future.

4. Conclusions and perspectives

In this review, we compare the silicon anodes with lithium metal anodes and other alloy anodes and explain the advantages of silicon-based anodes, as well as the formation and evolution of the SEI layer at the silicon anode/solid electrolyte interface. In addition, the application progress of silicon-based anodes in sulfide-based and other solid electrolyte-based all-solid-state batteries is introduced. Despite the considerable advances in the electrochemical performance of silicon-based anode all-solid-state batteries, there is still a considerable gap toward large-scale practical application. The SEI layer is formed due to the interfacial reaction between the silicon anode and the solid electrolyte, resulting in low initial Coulombic efficiency. And owing to the volume expansion and contraction of silicon during cycling, the SEI layer breaks and re-forms, resulting in silicon pulverization and rapid capacity decay. Therefore, constructing a flexible and strong silicon electrode/solid electrolyte interface helps to improve the cycling life of the silicon anode. Developing a new silicon anode with minimal expansion and new highly elastic and viscous binders will also facilitate the development of a robust composite anode.

Improving the initial Coulombic efficiency of the silicon anode could also help improve the specific capacity. Some strategies could be chosen, such as preparing pre-lithiated or coated silicon anode, and pairing with

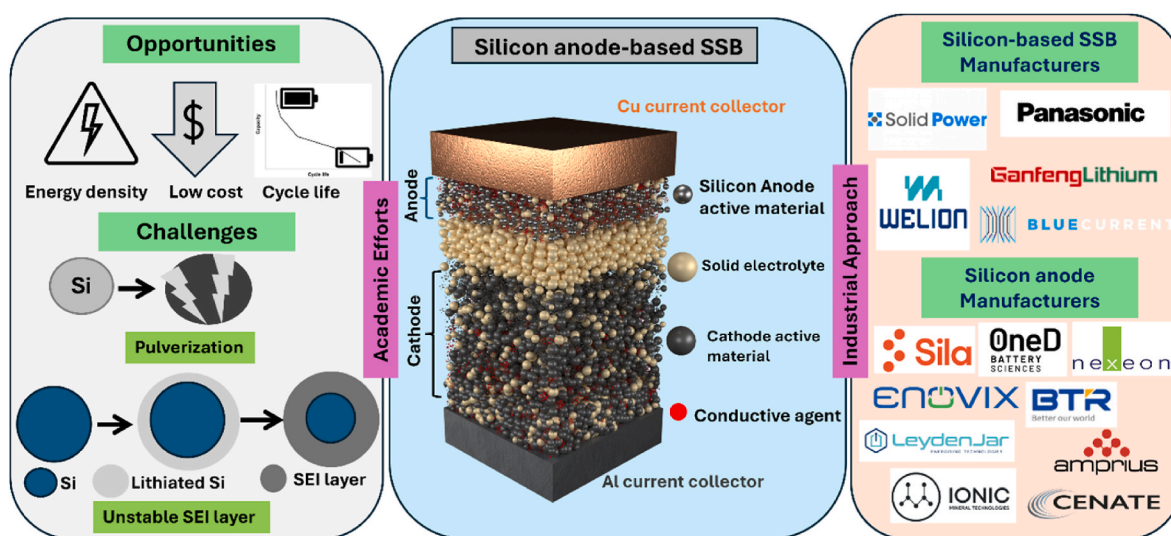


Fig. 7. An overview of Si anodes for SSB with opportunities and challenges and industrial manufacturers which effort on the development of Si-based anode manufacturers as well as Si-based SSB producers.

some solid electrolytes with good interfacial stability against silicon electrodes, such as $3\text{LiBH}_4\text{-LiI}$ with a low reduction potential.

Currently, the issue of low silicon active material loading in composite anode persists. In order to increase the areal capacity, it is necessary to reduce the content of inactive substances in the composite anode, including conductive carbon and solid electrolytes. Optimizing the particle size distribution and mass ratio of nano-silicon, conductive carbon, and sulfide electrolytes in the composite anode could help improve the areal capacity. Despite some reports in some literature that the use of pure micron silicon, columnar silicon, or silicon wafers with a specific orientation as anode could enhance the areal capacity, large cracks will still form in these batteries during the cycling even under higher stacking pressure. In the future, some strategies could be adopted, such as preparing a layer of carbon shell on the surface of porous silicon, or the use of hard carbon stabilized Li-Si alloy, or the use of Si/ Li_2Si_5 composite anode, etc., which will contribute to achieving high areal capacity while alleviating the volume expansion of silicon.

Reducing the volume change of silicon is very important for the long-term cycling stability of silicon-based solid-state batteries. One of the more typical methods is to apply a stacking pressure of more than 100 MPa to the battery. Although high stacking pressure will enhance capacity retention, it will simultaneously diminish the degree of lithiation, thereby reducing the charge and discharge capacity. Meanwhile, the necessity for bulky devices to implement such a substantial pressure will result in a reduction in the overall energy density of the cell. Therefore, it is essential to reduce the overall volume expansion/contraction of the composite anode through optimization of the silicon material and structure of the composite.

For example, preparing nano-porous silicon and uniformly mixing it with sulfide electrolyte and conductive carbon to prepare a composite anode could alleviate volume expansion. Furthermore, the silicon electrode could be coated or doped to mitigate the effects of volume change and facilitate the diffusion of lithium ions. The use of solid electrolytes with a relatively small elastic modulus, such as glassy electrolyte sulfide electrolyte, or organic-inorganic composite solid electrolyte, could accommodate the volume change of silicon during the cycling and ensure good interface contact between silicon anode and solid electrolyte. However, the room-temperature ionic conductivity of the majority of polymer-based composite electrolyte membranes is typically low. Therefore, improving the ionic conductivity and flexibility of the composite electrolyte membrane will help improve the rate performance of silicon-based all-solid-state batteries.

For the whole silicon-based all-solid-state battery, the thickness of the solid electrolyte layer needs to be reduced in the future. The majority of existing silicon-based cells use a sulfide electrolyte layer that is several hundred microns thick, which will greatly sacrifice the energy density of the entire cell. Developing an ultra-thin solid electrolyte layer with high room-temperature ionic conductivity, optimizing the N/P ratio and the composite electrode structure are of great significance for the ultimate realization of silicon-based all-solid-state batteries with high specific energy and long cycle life. To sustain and build better technologies towards a sustainable world for all, inventing environmentally responsible solutions and enabling the circular economy of SSB is mandatory. As the most promising energy storage system, there is still a long way to go in realizing the commercialization of SSB requirements of safety, energy density, and cycle stability.

CRedit authorship contribution statement

Palanivel Molaiyan: Writing – original draft, Conceptualization. **Buket Boz:** Writing – original draft, Conceptualization. **Glaydson Simoes dos Reis:** Writing – original draft. **Rafal Sliz:** Writing – original draft. **Shuo Wang:** Writing – original draft. **Marco Borsari:** Writing – original draft. **Ulla Lassi:** Writing – original draft. **Andrea Paoletta:** Writing – original draft, Conceptualization.

Declaration of competing interest

The authors declare that they have no known competing financial interests or personal relationships that could have appeared to influence the work reported in this paper.

Acknowledgments

A.P thanks the University of Modena and Reggio Emilia for allowing the publication of this review article in open access mode. P.M. gratefully acknowledges financial support from the Research Council of Finland (Academy Research Fellows 2024, Project In2BaT, grant no. 362298). G.S., R.S., and U.L. gratefully acknowledge the financial support of the EU/Interreg Aurora (Project GreenBattery, grant no. 20357574). Dr. Glaydson dos Simoes Reis gratefully acknowledges financial support from the Research Council of Finland (Academy Research Fellows 2024, Project: Bio-Adsorb&Energy, grant no. 361583). S.W. acknowledges the Natural Science Foundation of China (grant no. 52302305), Guangdong Basic and Applied Basic Research Foundation (Grant No. 2021A1515110312), Natural Science Foundation Exploration Program of Wuhan (Morning Light Plan) (grant no. 202401jc00089), and support from Tong Xiang Advanced New Materials Institute.

Data availability

No data was used for the research described in the article.

References

- [1] Tepe B, Jablonski S, Hesse H, Jossen A. Lithium-ion battery utilization in various modes of e-transportation. *ETransportation* 2023;18:100274. <https://doi.org/10.1016/j.etrans.2023.100274>.
- [2] Peng J, Zhao X, Ma J, Meng D, Zhu J, Zhang J, Yan S, Zhang K, Han Z. Enhancing lithium-ion battery monitoring: a critical review of diverse sensing approaches. *ETransportation* 2024;22:100360. <https://doi.org/10.1016/j.etrans.2024.100360>.
- [3] Armand M, Tarascon JM. Building better batteries. *Nature* 2008;451:652–7. <https://doi.org/10.1038/451652a>.
- [4] Chen R, Li Q, Yu X, Chen L, Li H. Approaching practically accessible solid-state batteries: stability issues related to solid electrolytes and interfaces. *Chem. Rev.* 2020;120:6820–77. <https://doi.org/10.1021/acs.chemrev.9b00268>.
- [5] Frith JT, Lacey MJ, Ulissi U. A non-academic perspective on the future of lithium-based batteries. *Nat Commun* 2023;14:420. <https://doi.org/10.1038/s41467-023-35933-2>.
- [6] Molaiyan P, Bhattacharyya S, dos Reis GS, Sliz R, Paoletta A, Lassi U. Towards greener batteries: sustainable components and materials for next-generation batteries. *Green Chem* 2024. <https://doi.org/10.1039/D3GC05027K>.
- [7] Wu D, Wu F. Toward better batteries: solid-state battery roadmap 2035+. *ETransportation* 2023;16:100224. <https://doi.org/10.1016/j.etrans.2022.100224>.
- [8] Cavers H, Molaiyan P, Abdollahifar M, Lassi U, Kwade A. Perspectives on improving the safety and sustainability of high voltage lithium-ion batteries through the electrolyte and separator region. *Adv Energy Mater* 2022;12:2200147. <https://doi.org/10.1002/aenm.202200147>.
- [9] Molaiyan P, Mailhot SE, Voges K, Kantola AM, Hu T, Michalowski P, Kwade A, Telkki V-V, Lassi U. Investigation of the structure and ionic conductivity of a Li_3InCl_6 modified by dry room annealing for solid-state Li-ion battery applications. *Mater Des* 2023;227:111690. <https://doi.org/10.1016/j.matdes.2023.111690>.
- [10] Wu Y, Feng X, Ma Z, Gao L, Wang Y, Zhao C-Z, Ren D, Yang M, Xu C, Wang L, He X, Lu L, Ouyang M. Electrolyte design for stable electrode-electrolyte interphase to enable high-safety and high-voltage batteries. *ETransportation* 2023;15:100216. <https://doi.org/10.1016/j.etrans.2022.100216>.
- [11] Kim M, Ahn H, Choi J, Kim WB. A rational design of silicon-based anode for all-solid-state lithium-ion batteries: a review. *Energy Technol* 2023;11:2201321. <https://doi.org/10.1002/ente.202201321>.
- [12] Cao D, Sun X, Li Y, Anderson A, Lu W, Zhu H. Long-cycling sulfide-based all-solid-state batteries enabled by electrochemo-mechanically stable electrodes. *Adv. Mater.* 2022;34:2200401. <https://doi.org/10.1002/adma.202200401>.
- [13] Zhan X, Li M, Li S, Pang X, Mao F, Wang H, Sun Z, Han X, Jiang B, He Y-B, Li M, Zhang Q, Zhang L. Challenges and opportunities towards silicon-based all-solid-state batteries. *Energy Storage Mater* 2023;61:102875. <https://doi.org/10.1016/j.ensm.2023.102875>.
- [14] Leblanc D, Guerfi A, Cho M, Paoletta A, Wang Y, Mauger A, Julien C, Zaghib K. In: Kumta PN, Hepp AF, Datta MK, Velikokhatnyi OIBT-SAS for L-IB, editors. Chapter 11 - advanced silicon-based electrodes for high-energy lithium-ion batteries.

- Elsevier; 2022. p. 411–56. <https://doi.org/10.1016/B978-0-12-819660-1.00005-0>.
- [15] Hopcroft MA, Nix WD, Kenny TW. What is the young's modulus of silicon? *J Microelectromech Syst* 2010;19:229–38. <https://doi.org/10.1109/JMEMS.2009.2039697>.
- [16] Wang Y, Liu T, Kumar J. Effect of pressure on lithium metal deposition and stripping against sulfide-based solid electrolytes. *ACS Appl Mater Interfaces* 2020;12:34771–6. <https://doi.org/10.1021/acsmi.0c06201>.
- [17] Doux J-M, Nguyen H, Tan DHS, Banerjee A, Wang X, Wu EA, Jo C, Yang H, Meng YS. Stack pressure considerations for room-temperature all-solid-state lithium metal batteries. *Adv Energy Mater* 2020;10:1903253. <https://doi.org/10.1002/aenm.201903253>.
- [18] Wu J, Liu S, Han F, Yao X, Wang C. Lithium/sulfide all-solid-state batteries using sulfide electrolytes. *Adv. Mater.* 2021;33:2000751. <https://doi.org/10.1002/adma.202000751>.
- [19] Kim JY, Jung S, Kang SH, Park J, Lee MJ, Jin D, Shin DO, Lee Y-G, Lee YM. Graphite-silicon diffusion-dependent electrode with short effective diffusion length for high-performance all-solid-state batteries. *Adv Energy Mater* 2022;12:2103108. <https://doi.org/10.1002/aenm.202103108>.
- [20] Lewis JA, Cavallaro KA, Liu Y, McDowell MT. The promise of alloy anodes for solid-state batteries. *Joule* 2022;6:1418–30. <https://doi.org/10.1016/j.joule.2022.05.016>.
- [21] Liu C, Sun J, Zheng P, Jiang L, Liu H, Chai J, Liu Q, Liu Z, Zheng Y, Rui X. Recent advances of non-lithium metal anode materials for solid-state lithium-ion batteries. *J Mater Chem A* 2022;10:16761–78. <https://doi.org/10.1039/D2TA03905B>.
- [22] Yubuchi S, Nakamura W, Bibienne T, Rousselot S, Taylor LW, Pasquali M, Dollé M, Sakuda A, Hayashi A, Tatsumisago M. All-solid-state cells with Li₄Ti₅O₁₂/carbon nanotube composite electrodes prepared by infiltration with argyrodite sulfide-based solid electrolytes via liquid-phase processing. *J Power Sources* 2019;417:125–31. <https://doi.org/10.1016/j.jpowsour.2019.01.070>.
- [23] Oh DY, Kim DH, Jung SH, Han J-G, Choi N-S, Jung YS. Single-step wet-chemical fabrication of sheet-type electrodes from solid-electrolyte precursors for all-solid-state lithium-ion batteries. *J Mater Chem A* 2017;5:20771–9. <https://doi.org/10.1039/C7TA06873E>.
- [24] Ito S, Fujiki S, Yamada T, Aihara Y, Park Y, Kim TY, Baek S-W, Lee J-M, Doo S, Machida N. A rocking chair type all-solid-state lithium ion battery adopting Li₂O-ZrO₂ coated LiNi_{0.8}Co_{0.15}Al_{0.05}O₂ and a sulfide based electrolyte. *J Power Sources* 2014;248:943–50. <https://doi.org/10.1016/j.jpowsour.2013.10.005>.
- [25] Ping W, Yang C, Bao Y, Wang C, Xie H, Hitz E, Cheng J, Li T, Hu L. A silicon anode for garnet-based all-solid-state batteries: interfaces and nanomechanics. *Energy Storage Mater* 2019;21:246–52. <https://doi.org/10.1016/j.ensm.2019.06.024>.
- [26] Sakuma M, Suzuki K, Hirayama M, Kanno R. Reactions at the electrode/electrolyte interface of all-solid-state lithium batteries incorporating Li-M (M=Sn, Si) alloy electrodes and sulfide-based solid electrolytes. *Solid State Ionics* 2016;285:101–5. <https://doi.org/10.1016/j.ssi.2015.07.010>.
- [27] Zhang H, Mao C, Li J, Chen R. Advances in electrode materials for Li-based rechargeable batteries. *RSC Adv* 2017;7:33789–811. <https://doi.org/10.1039/C7RA04370H>.
- [28] dos Reis GS, Molaiyan P, Subramaniam CM, García-Alvarado F, Paoletta A, de Oliveira HP, Lassi U. Biomass-derived carbon-silicon composites (C@Si) as anodes for lithium-ion and sodium-ion batteries: a promising strategy towards long-term cycling stability: a mini review. *Electrochem Commun* 2023;153:107536. <https://doi.org/10.1016/j.elecom.2023.107536>.
- [29] Boz B, Fröhlich K, Neidhardt L, Molaiyan P, Bertoni G, Ricci M, De Boni F, Vuksanovic M, Romio M, Whitmore K, Jahn M. Evaluating polyacrylic acid as a universal aqueous binder for Ni-rich cathodes NMC811 and Si anodes in full cell lithium-ion batteries. *Chempluschem n/a* 2024:e202400195. <https://doi.org/10.1002/cplu.202400195>.
- [30] Molaiyan P, Abdollahifar M, Boz B, Beutl A, Krammer M, Zhang N, Tron A, Romio M, Ricci M, Adelung R, Kwade A, Lassi U, Paoletta A. Optimizing current collector interfaces for efficient “anode-free” lithium metal batteries. *Adv. Funct. Mater.* n/a 2023:2311301. <https://doi.org/10.1002/adfm.202311301>.
- [31] Nitta N, Yushin G. High-capacity anode materials for lithium-ion batteries: choice of elements and structures for active particles. *Part. Part. Syst. Charact.* 2014;31:317–36. <https://doi.org/10.1002/ppsc.201300231>.
- [32] Molaiyan P, Dos Reis GS, Karuppiyah D, Subramaniam CM, García-Alvarado F, Lassi U. Recent progress in biomass-derived carbon materials for Li-ion and Na-ion batteries—a review. *Batteries* 2023;9. <https://doi.org/10.3390/batteries9020116>.
- [33] Aryanfar A, Brooks DJ, Colussi AJ, Hoffmann MR. Quantifying the dependence of dead lithium losses on the cycling period in lithium metal batteries. *Phys Chem Chem Phys* 2014;16:24965–70. <https://doi.org/10.1039/C4CP03590A>.
- [34] Howlett PC, MacFarlane DR, Hollenkamp AF. A sealed optical cell for the study of lithium-electrode|electrolyte interfaces. *J Power Sources* 2003;114:277–84. [https://doi.org/10.1016/S0378-7753\(02\)00603-1](https://doi.org/10.1016/S0378-7753(02)00603-1).
- [35] Wang Q, Liu B, Shen Y, Wu J, Zhao Z, Zhong C, Hu W. Confronting the challenges in lithium anodes for lithium metal batteries. *Adv Sci* 2021;8:2101111. <https://doi.org/10.1002/advs.202101111>.
- [36] Kushima A, So KP, Su C, Bai P, Kuriyama N, Maebashi T, Fujiwara Y, Bazant MZ, Li J. Liquid cell transmission electron microscopy observation of lithium metal growth and dissolution: root growth, dead lithium and lithium flotsams. *Nano Energy* 2017;32:271–9. <https://doi.org/10.1016/j.nanoen.2016.12.001>.
- [37] Harry KJ, Hallinan DT, Parkinson DY, MacDowell AA, Balsara NP. Detection of subsurface structures underneath dendrites formed on cycled lithium metal electrodes. *Nat Mater* 2014;13:69–73. <https://doi.org/10.1038/nmat3793>.
- [38] McDowell MT, Lee SW, Nix WD, Cui Y. 25th anniversary article: understanding the lithiation of silicon and other alloying anodes for lithium-ion batteries. *Adv. Mater.* 2013;25:4966–85. <https://doi.org/10.1002/adma.201301795>.
- [39] Parikh P, Sina M, Banerjee A, Wang X, D'Souza MS, Doux J-M, Wu EA, Trieu OY, Gong Y, Zhou Q, Snyder K, Meng YS. Role of polyacrylic acid (PAA) binder on the solid electrolyte interphase in silicon anodes. *Chem Mater* 2019;31:2535–44. <https://doi.org/10.1021/acs.chemmater.8b05020>.
- [40] Sun Z, Yin Q, Chen H, Li M, Zhou S, Wen S, Pan J, Zheng Q, Jiang B, Liu H, Kim K, Li J, Han X, He Y-B, Zhang L, Li M, Zhang Q. Building better solid-state batteries with silicon-based anodes. *Interdiscip. Mater.* 2023;2:635–63. <https://doi.org/10.1002/idm.212111>.
- [41] Poetke S, Hippauf F, Baasner A, Dörfler S, Althues H, Kaskel S. Nanostructured Si—C composites as high-capacity anode material for all-solid-state lithium-ion batteries. *Batter. Supercaps* 2021;4:1323–34. <https://doi.org/10.1002/batt.202100055>.
- [42] Goodenough JB, Park KS. The Li-ion rechargeable battery: a perspective. *J Am Chem Soc* 2013;135:1167–76. <https://doi.org/10.1021/ja3091438>.
- [43] Sina M, Alvarado J, Shobukawa H, Alexander C, Manichev V, Feldman L, Gustafsson T, Stevenson KJ, Meng YS. Direct visualization of the solid electrolyte interphase and its effects on silicon electrochemical performance. *Adv Mater Interfac* 2016;3:1600438. <https://doi.org/10.1002/admi.201600438>.
- [44] Huo H, Jiang M, Bai Y, Ahmed S, Volz K, Hartmann H, Henss A, Singh CV, Raabe D, Janek J. Chemo-mechanical failure mechanisms of the silicon anode in solid-state batteries. *Nat Mater* 2024;23:543–51. <https://doi.org/10.1038/s41563-023-01792-x>.
- [45] Han X, Gu L, Sun Z, Chen M, Zhang Y, Luo L, Xu M, Chen S, Liu H, Wan J, He Y-B, Chen J, Zhang Q. Manipulating charge-transfer kinetics and a flow-domain LiF-rich interphase to enable high-performance microsilicon-silver-carbon composite anodes for solid-state batteries. *Energy Environ Sci* 2023;16:5395–408. <https://doi.org/10.1039/D3EE01696J>.
- [46] Gu L, Han J, Chen M, Zhou W, Wang X, Xu M, Lin H, Liu H, Chen H, Chen J, Zhang Q, Han X. Enabling robust structural and interfacial stability of micron-Si anode toward high-performance liquid and solid-state lithium-ion batteries. *Energy Storage Mater* 2022;52:547–61. <https://doi.org/10.1016/j.ensm.2022.08.028>.
- [47] Liu N, Wu H, McDowell MT, Yao Y, Wang C, Cui Y. A yolk-shell design for stabilized and scalable Li-ion battery alloy anodes. *Nano Lett* 2012;12:3315–21. <https://doi.org/10.1021/nl3014814>.
- [48] Wu H, Zheng G, Liu N, Carney TJ, Yang Y, Cui Y. Engineering empty space between Si nanoparticles for lithium-ion battery anodes. *Nano Lett* 2012;12:904–9. <https://doi.org/10.1021/nl203967r>.
- [49] Guo K, Kumar R, Xiao X, Sheldon BW, Gao H. Failure progression in the solid electrolyte interphase (SEI) on silicon electrodes. *Nano Energy* 2020;68:104257. <https://doi.org/10.1016/j.nanoen.2019.104257>.
- [50] Li J, Dudney NJ, Nanda J, Liang C. Artificial solid electrolyte interphase to address the electrochemical degradation of silicon electrodes. *ACS Appl Mater Interfaces* 2014;6:10083–8. <https://doi.org/10.1021/am5009419>.
- [51] Lee YM, Lee JY, Shim H-T, Lee JK, Park J-K. SEI layer formation on amorphous Si thin electrode during pre-cycling. *J Electrochem Soc* 2007;154:A515. <https://doi.org/10.1149/1.2719644>.
- [52] Lu P, Li C, Schneider EW, Harris SJ. Chemistry, impedance, and morphology evolution in solid electrolyte interphase films during formation in lithium ion batteries. *J Phys Chem C* 2014;118:896–903. <https://doi.org/10.1021/jp4111019>.
- [53] Cresce Av, Russell SM, Baker DR, Gaskell KJ, Xu K. In situ and quantitative characterization of solid electrolyte interphases. *Nano Lett* 2014;14:1405–12. <https://doi.org/10.1021/nl404471v>.
- [54] Philippe B, Dedryvère R, Allouche J, Lindgren F, Gorgoi M, Rensmo H, Gonbeau D, Edström K. Nanosilicon electrodes for lithium-ion batteries: interfacial mechanisms studied by hard and soft X-ray photoelectron spectroscopy. *Chem Mater* 2012;24:1107–15. <https://doi.org/10.1021/cm2034195>.
- [55] Han X, Wang S, Xu Y, Zhong G, Zhou Y, Liu B, Jiang X, Wang X, Li Y, Zhang Z, Chen S, Wang C, Yang Y, Zhang W, Wang J, Liu J, Yang J. All solid thick oxide cathodes based on low temperature sintering for high energy solid batteries. *Energy Environ Sci* 2021;14:5044–56. <https://doi.org/10.1039/D1EE01494C>.
- [56] Campanella D, Belanger D, Paoletta A. Beyond garnets, phosphates and phosphosulfides solid electrolytes: new ceramic perspectives for all solid lithium metal batteries. *J Power Sources* 2021;482:228949. <https://doi.org/10.1016/j.jpowsour.2020.228949>.
- [57] Wang X, He K, Li S, Zhang J, Lu Y. Realizing high-performance all-solid-state batteries with sulfide solid electrolyte and silicon anode: a review. *Nano Res* 2023;16:3741–65. <https://doi.org/10.1007/s12274-022-4526-9>.
- [58] Ren D, Lu L, Hua R, Zhu G, Liu X, Mao Y, Rui X, Wang S, Zhao B, Cui H, Yang M, Shen H, Zhao C-Z, Wang L, He X, Liu S, Hou Y, Tan T, Wang P, Nitta Y, Ouyang M. Challenges and opportunities of practical sulfide-based all-solid-state batteries. *ETransportation* 2023;18:100272. <https://doi.org/10.1016/j.etrans.2023.100272>.
- [59] Cervera RB, Suzuki N, Ohnishi T, Osada M, Mitsuishi K, Kambara T, Takada K. High performance silicon-based anodes in solid-state lithium batteries. *Energy Environ Sci* 2014;7:662–6. <https://doi.org/10.1039/C3EE43306D>.
- [60] Cangaz S, Hippauf F, Reuter FS, Doerfler S, Abendroth T, Althues H, Kaskel S. Enabling high-energy solid-state batteries with stable anode interphase by the use

- of columnar silicon anodes. *Adv Energy Mater* 2020;10:2001320. <https://doi.org/10.1002/aenm.202001320>.
- [61] Zhang F, Guo Y, Zhang L, Jia P, Liu X, Qiu P, Zhang H, Huang J. A review of the effect of external pressure on all-solid-state batteries. *ETransportation* 2023;15:100220. <https://doi.org/10.1016/j.etrans.2022.100220>.
- [62] Tan DHS, Chen Y-T, Yang H, Bao W, Sreemanyan B, Doux J-M, Li W, Lu B, Ham S-Y, Sayahpour B, Scharf J, Wu EA, Deysheer G, Han HE, Hah HJ, Jeong H, Lee JB, Chen Z, Meng YS. Carbon-free high-loading silicon anodes enabled by sulfide solid electrolytes. *Science* 2021;373:1494–9. <https://doi.org/10.1126/science.abg7217> (80).
- [63] Xu X, Sun Q, Li Y, Ji F, Cheng J, Zhang H, Zeng Z, Rao Y, Liu H, Li D, Ci L. Nano silicon anode without electrolyte adding for sulfide-based all-solid-state lithium-ion batteries. *Small n/a* 2023;2302934. <https://doi.org/10.1002/sml.202302934>.
- [64] Pan J, Peng H, Yan Y, Bai Y, Yang J, Wang N, Dou S, Huang F. Solid-state batteries designed with high ion conductive composite polymer electrolyte and silicon anode. *Energy Storage Mater* 2021;43:165–71. <https://doi.org/10.1016/j.ensm.2021.09.001>.
- [65] Cao D, Ji T, Singh A, Bak S, Du Y, Xiao X, Xu H, Zhu J, Zhu H. Unveiling the mechanical and electrochemical evolution of nanosilicon composite anodes in sulfide-based all-solid-state batteries. *Adv Energy Mater* 2023;13:2203969. <https://doi.org/10.1002/aenm.202203969>.
- [66] Huang Y, Shao B, Wang Y, Han F. Solid-state silicon anode with extremely high initial coulombic efficiency. *Energy Environ Sci* 2023;16:1569–80. <https://doi.org/10.1039/D2EE04057C>.
- [67] Grandjean M, Pichardo M, Biecher Y, Haon C, Chenevier P. Matching silicon-based anodes with sulfide-based solid-state electrolytes for Li-ion batteries. *J Power Sources* 2023;580:233386. <https://doi.org/10.1016/j.jpowsour.2023.233386>.
- [68] Yamamoto M, Terauchi Y, Sakuda A, Kato A, Takahashi M. Effects of volume variations under different compressive pressures on the performance and microstructure of all-solid-state batteries. *J Power Sources* 2020;473:228595. <https://doi.org/10.1016/j.jpowsour.2020.228595>.
- [69] Famprikis T, Canepa P, Dawson JA, Islam MS, Masquelier C. Fundamentals of inorganic solid-state electrolytes for batteries. *Nat Mater* 2019;18:1278–91. <https://doi.org/10.1038/s41563-019-0431-3>.
- [70] Dunlap NA, Kim J, Guthery H, Jiang C-S, Morrissey I, Stoldt CR, Oh KH, Al-Jassim M, Lee S-H. Towards the commercialization of the all-solid-state Li-ion battery: local bonding structure and the reversibility of sheet-style Si-PAN anodes. *J Electrochem Soc* 2020;167:60522. <https://doi.org/10.1149/1945-7111/ab84fc>.
- [71] Kim DH, Lee HA, Song YB, Park JW, Lee S-M, Jung YS. Sheet-type Li₆PS₅Cl-infiltrated Si anodes fabricated by solution process for all-solid-state lithium-ion batteries. *J Power Sources* 2019;426:143–50. <https://doi.org/10.1016/j.jpowsour.2019.04.028>.
- [72] Kim J, Kim C, Jang I, Park J, Kim J, Paik U, Song T. Si nanoparticles embedded in carbon nanofiber sheathed with Li₆PS₅Cl as an anode material for all-solid-state batteries. *J Power Sources* 2021;510:230425. <https://doi.org/10.1016/j.jpowsour.2021.230425>.
- [73] Jun S, Lee G, Song YB, Lim H, Baek KH, Lee ES, Kim JY, Kim DW, Park JH, Jung YS. Interlayer engineering and prelithiation: empowering Si anodes for low-pressure-operating all-solid-state batteries. *Small n/a* 2024;2309437. <https://doi.org/10.1002/sml.202309437>.
- [74] Grandjean M, Perrey M, Randraema X, Laurier J, Chenevier P, Haon C, Liatard S. Low pressure cycling of solid state Li-ion pouch cells based on NMC – sulfide – Nanosilicon chemistry. *J Power Sources* 2023;585:233646. <https://doi.org/10.1016/j.jpowsour.2023.233646>.
- [75] Wang Y, Li X. Fast kinetics design for solid-state battery device. *Adv. Mater.* 2024; 36:2309306. <https://doi.org/10.1002/adma.202309306>.
- [76] Liu X, Wang D, Wang X, Wang D, Li Y, Fu J, Zhang R, Liu Z, Zhou Y, Wen G. Designing compatible ceramic/polymer composite solid-state electrolyte for stable silicon nanosheet anodes. *Small n/a* 2024;2309724. <https://doi.org/10.1002/sml.202309724>.
- [77] Na I, Kim H, Kunze S, Nam C, Jo S, Choi H, Oh S, Choi E, Song YB, Jung YS, Lee YS, Lim J. Monolithic 100% silicon wafer anode for all-solid-state batteries achieving high areal capacity at room temperature. *ACS Energy Lett* 2023;8:1936–43. <https://doi.org/10.1021/acsenerylett.3c00496>.
- [78] Fan Z, Ding B, Li Z, Chang Z, Hu B, Xu C, Zhang X, Dou H, Zhang X. In-situ prelithiation of electrolyte-free silicon anode for sulfide all-solid-state batteries. *ETransportation* 2023;18:100277. <https://doi.org/10.1016/j.etrans.2023.100277>.
- [79] Poetke S, Cangaz S, Hippauf F, Haufe S, Dörfler S, Althues H, Kaskel S. Partially lithiated microscale silicon particles as anode material for high-energy solid-state lithium-ion batteries. *Energy Technol* 2023;11:2201330. <https://doi.org/10.1002/ente.202201330>.
- [80] Rana M, Rudel Y, Heuer P, Schlaumann E, Rosenbach C, Ali MY, Wiggers H, Bielefeld A, Zeier WG. Toward achieving high areal capacity in silicon-based solid-state battery anodes: what influences the rate-performance? *ACS Energy Lett* 2023;8:3196–203. <https://doi.org/10.1021/acsenerylett.3c00722>.
- [81] Balaiash M, Gonzalez-Rosillo JC, Kim KJ, Zhu Y, Hood ZD, Rupp JLM. Processing thin but robust electrolytes for solid-state batteries. *Nat Energy* 2021;6:227–39. <https://doi.org/10.1038/s41560-020-00759-5>.
- [82] Zhao N, Khokhar W, Bi Z, Shi C, Guo X, Fan LZ, Nan CW. Solid garnet batteries. *Joule* 2019;3:1190–9. <https://doi.org/10.1016/j.joule.2019.03.019>.
- [83] Molaiyan P, Valikangas J, Sliz R, Ramteke DD, Hu T, Paoletta A, Fabritius T, Lassi U. Screen-printed composite LiFePO₄-LLZO cathodes towards solid-state Li-ion batteries. *Chemelectrochem* 2024;11:e202400051. <https://doi.org/10.1002/celc.202400051>.
- [84] Göttlinger M, Amrhein S, Piesold C, Weller M, Peters S, Giffin GA. Development of silicon polymer electrodes with a hybrid polymer electrolyte for all-solid-state lithium-ion batteries. *J Electrochem Soc* 2023;170:30541. <https://doi.org/10.1149/1945-7111/acc697>.
- [85] Zhou L, Zuo T, Li C, Zhang Q, Janek J, Nazar LF. Li₃-xZrx(Ho/Lu)_{1-x}Cl₆ solid electrolytes enable ultrahigh-loading solid-state batteries with a prelithiated Si anode. *ACS Energy Lett* 2023;8:3102–11. <https://doi.org/10.1021/acsenerylett.3c00763>.
- [86] Han SY, Lee C, Lewis JA, Yeh D, Liu Y, Lee H-W, McDowell MT. Stress evolution during cycling of alloy-anode solid-state batteries. *Joule* 2021;5:2450–65. <https://doi.org/10.1016/j.joule.2021.07.002>.
- [87] Zeng B, Gu Q, Zhang Y, Wang M, Gao J, Fan C, Tang W. Engineering electrode–electrolyte interface for ultrastable Si-based solid-state batteries. *Surface Interfac* 2024;44:103687. <https://doi.org/10.1016/j.surfin.2023.103687>.
- [88] Han X, Xu M, Gu LH, Lan CF, Chen MF, Lu JJ, Sheng BF, Wang P, Chen SY, Chen JZ. Monolithic and conductive network and mechanical stress releasing layer on micron-silicon anode enabling high-energy solid-state battery. *Rare Met* 2024;43:1017–29. <https://doi.org/10.1007/s12598-023-02498-4>.
- [89] Zhang L, Lin Y, Peng X, Wu M, Zhao T. A high-capacity polyethylene oxide-based all-solid-state battery using a metal–organic framework hosted silicon anode. *ACS Appl Mater Interfaces* 2022;14:24798–805. <https://doi.org/10.1021/acsaami.2c04487>.
- [90] Zhang Z, Sun Z, Han X, Liu Y, Pei S, Li Y, Luo L, Su P, Lan C, Zhang Z, Xu S, Guo S, Huang W, Chen S, Wang M-S. An all-electrochem-active silicon anode enabled by spontaneous Li–Si alloying for ultra-high performance solid-state batteries. *Energy Environ Sci* 2024;17:1061–72. <https://doi.org/10.1039/D3EE03877G>.
- [91] Cao D, Sun X, Wang Y, Zhu H. Bipolar stackings high voltage and high cell level energy density sulfide based all-solid-state batteries. *Energy Storage Mater* 2022; 48:458–65. <https://doi.org/10.1016/j.ensm.2022.03.012>.
- [92] Yan W, Mu Z, Wang Z, Huang Y, Wu D, Lu P, Lu J, Xu J, Wu Y, Ma T, Yang M, Zhu X, Xia Y, Shi S, Chen L, Li H, Wu F. Hard-carbon-stabilized Li–Si anodes for high-performance all-solid-state Li-ion batteries. *Nat Energy* 2023;8:800–13. <https://doi.org/10.1038/s41560-023-01279-8>.
- [93] Ionic mineral technologies, (n.d.).
- [94] nexenglobal, (n.d.).
- [95] Amprius technology, (n.d.).
- [96] BTR China, (n.d.).
- [97] WeLion, [https://www.Solidstatelion.com/En/\(n.d.\)](https://www.Solidstatelion.com/En/(n.d.)).
- [98] Gotion, [https://www.Gotion.com.cn/News/Companydetails/1294.html\(n.d.\)](https://www.Gotion.com.cn/News/Companydetails/1294.html(n.d.)).
- [99] GAC Group, [https://www.Gac.Com.Cn/Cn/News/Detail?Baseid=18762\(n.d.\)](https://www.Gac.Com.Cn/Cn/News/Detail?Baseid=18762(n.d.)).
- [100] Solid Power, [https://www.Solidpowerbattery.com/All-Solid-State-Batteries/Default.aspx\(n.d.\)](https://www.Solidpowerbattery.com/All-Solid-State-Batteries/Default.aspx(n.d.)).